Reprinted from JOURNAL OF APPLIED MECHANICS, *Vol. 45, No. 2, June 1978*

B. Budiansky
Professor. Mem. ASME

J. W. Hutchinson
Professor. Mem. ASME

Division of Applied Sciences,
Harvard University,
Cambridge, Mass.

Analysis of Closure in Fatigue Crack Growth

A theoretical study is made of the implicotions of a Dugdole-Barenblatt model for fatigue crack growth under steady cyclic loading. Residual plastic stretches and the effects of crack closure on crack opening and closing loads are calculated by complex function methods for a range of loading ratios. An assessment is made of the influence of cyclic strain hardening and softening.

Introduction

This paper presents a theoretical model for the phenomenon of fatigue-crack-closure discovered experimentally by Elber [1, 2][1] and explores some of its analytical consequences. The theory comtemplates the steady-state growth of a long crack under the assumptions of small-scale yielding according to the ideally-plastic Dugdale-Barenblatt model. Function-analytic methods are used to derive plastic wake residual stretches and crack opening loads as functions of the applied load range.

Earlier calculations of this kind have been executed by finite-element methods [3–5]. A recent analytic study [6] is based on an assumed size for the plastic wake stretch, in contrast to the present work in which this stretch magnitude is an outcome of the calculation. In [7, 8] the Dugdale model was used to make an integral equation formulatiun of the closure conditions, which were then used to estimate closure contact stresses and reduced effective stress intensity factors. Finally, Paris [9] has made an ingenious engineering calculation that incorporates the essential features of the closure phenomenon in an approximate, ad hoc fashion.

We note that the Dugdale model is most appropriate for plane stress problems, whereas plane strain conditions are generally more relevant to fatigue crack growth. For this reason, we do not propose to explore the implications of the present model to great depth.

Theoretical Model

We consider a $2D$, Mode I craek (Fig. 1(a)) and invoke the assumptions of small-scale yielding. This means that the region of plastic deformation is so small that the asymptotic *elastic* crack-tip stress distribution given by

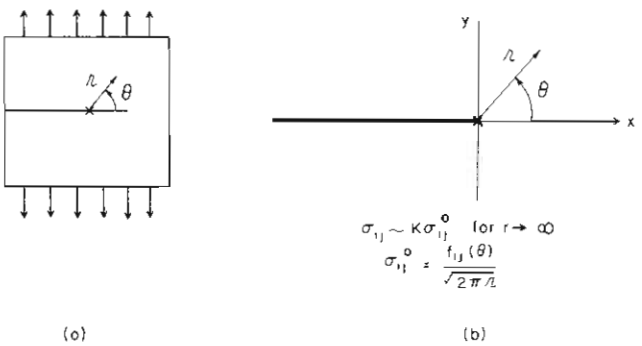

Fig. 1 Crack-tip asymptotics

$$\sigma_{ij}^E = \frac{Kf_{ij}(\theta)}{\sqrt{2\pi r}} \equiv K\sigma_{ij}^0 \tag{1}$$

stays accurate at distances r that are large compared to the plastic zone size. In (1), K is the conventional elastic stress-intensity factor that would be obtained in the absence of plasticity, and may be regarded as a prescribed applied load parameter. Small-scale yielding crack-tip analysis then proceeds on the basis of the geometry of Fig. 1(b), wherein the crack lies along the negative x-axis, the stresses are presumed asymptotic to (1) for $r \to \infty$, and appropriate constitutive relations and crack boundary conditions are invoked.

Under the Dugdale-Barenblatt hypothesis, all plastic deformation is confined to an infinitesimally thin zone along the x-axis, which may undergo an arbitrary stretch $\delta(x)$ in the y-direction whenever the stress σ_y reaches the ideally plastic tensile yield stress σ_Y. Coupled with the assumption that compressive crushing (negative stretch) occurs at the compressive yield stress, and that all stresses must remain bounded, the Dugdale model permits the formulation of well-set bonndary-value problems of plane elasticity for the determination of the plastic stretch distribution, and, as will be shown, the residual plastic stretches lefl in the wake of a growing fatigue crack.

[1] Numbers in brackets designate References at end of paper.

Contributed by the Applied Mecbanics Division for publication in the JOURNAL OF APPLIED MECHANICS.

Discussion on this paper should be addressed to the Editorial Department, ASME, United Engineering Center, 345 East 47th Street, New York, N. Y. 10017, and will be accepted until September 1, 1978. Readers who need more time to prepare a discussion should request an extension of the deadline from the Editorial Department. Mannscript received by ASME Applied Mechanics Division, June, 1977; final revision, October, 1977.

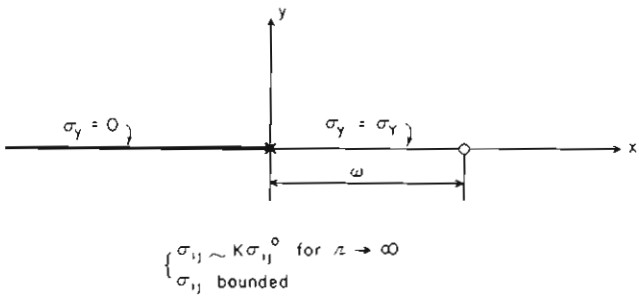

Fig. 2 Dugdale problem formulation, stationary crack

Analysis and Results

Stationary Crack. The well-known Dugdale solution for the single loading of a stationary crack, given by the bounded plane elasticity solution of the problem formulation of Fig. 2, provides the result [10]

$$w = (\pi/8)(K/\sigma_Y)^2 \tag{2}$$

for the plastic-yielding zone size. For plane-stress, the crack-tip opening displacement is given by

$$\delta_0 = K^2/E\sigma_Y = 8\sigma_Y w/(\pi E) \tag{3}$$

and the plastic stretch variation in $(0, w)$ is given by

$$\delta/\delta_0 = g(x/w) \tag{4}$$

where

$$g(\xi) = \sqrt{1-\xi} - \frac{\xi}{2}\log\left|\frac{1+\sqrt{1-\xi}}{1-\sqrt{1-\xi}}\right| \tag{5}$$

For $x < 0$, the same expression for δ/δ_0 provides the crack opening displacement, as illustrated in Fig. 3(a).

To provide further perspective to the subsequent crack-growth analysis, we reproduce the known result [10] for unloading the stationary crack to $K_{min} = 0$. If reverse plastic flow may occur under compressive stresses $\sigma_y = -\sigma_Y$, the compressive yield zone at $K_{min} = 0$ lies in the interval $(0, w/4)$. The formula

$$\delta/\delta_0 = g(x/w) - \frac{1}{2}g(4x/w) \tag{6}$$

gives the residual plastic stretch in this interval, and also provides the residual crack opening at $K = 0$ for $x < 0$, as illustrated in Fig. 3(b). In the interval $(w/4, w)$, the plastic stretch δ_M that was produced by K_{max} remains unchanged. Note that the crack-tip stretch is reduced to half the value it had at $K = K_{max}$.

Under cyclic loading between $K = K_{max}$ and $K = 0$, the stationary crack oscillates between the configurations of Figs. 3(a and b). It is evident, however, that a growing crack under the same cyclic loading must experience quite different crack-tip deformations. As the crack grows, it leaves in its wake plastically stretched material that, in our model, remains appended to the upper and lower surfaces of the crack as the crack tip penetrates the stretched material ahead of the crack. The total thickness of these stretched appendages just behind the crack tip must equal the plastic stretch just ahead of the tip at $K = K_{min}$. Clearly, the configuration of Fig. 3(b) is not consistent with this process, because the crack opeuing displacements behind the crack tip are too small to accommodate the residual stretch. The stretched material attached to the crack surfaces will necessarily make contact before the unloaded state is reached. This is the essence of the crack closure phenomenon; its detailed analysis follows, first for the case $K_{min} = 0$.

Growing Crack ($K_{min} = 0$). The stationary-crack states shown in Figs. 3(a,b) for K_{max} and $K_{min} = 0$ are replaced by those in Figs. 4(a,b) for the crack growing under cyclic loading. We assume an idealized steady-state situation: the crack has always been growing under

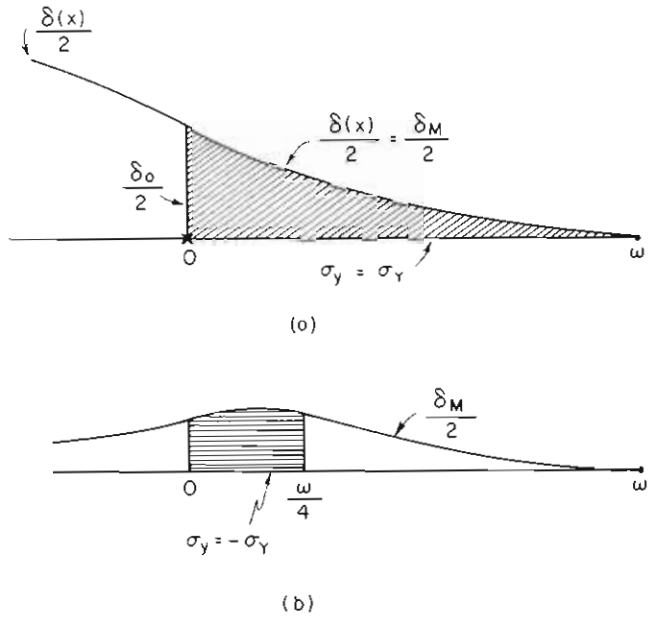

Fig. 3 Dugdale model, stationary crack: (a) $K = K_{max}$ and (b) unloading to $K = 0$

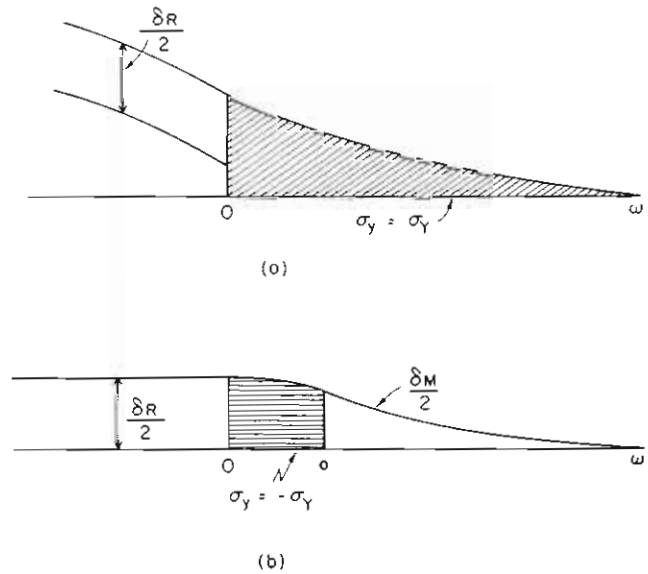

Fig. 4 Growing crack: (a) $K = K_{max}$ and (b) $K = K_{min} = 0$

constant K_{max}. At $K = K_{max}$, Fig. 4(a) is the same as Fig. 3(a) except for the residually stretched material of as-yet-unknown size $\delta_R/2$ at the upper and lower crack surfaces. In Fig. 4(b), we suppose that the plastically stretched upper and lower crack surfaces are in contact all along their lengths; that there is a region ahead of the crack tip, of unknown length a, that has gone into reverse plastic flow, leading to a total crack tip residual strain equal to δ_R; and that between $x = a$ aud $x = w$ the plastic stretch δ_M that existed at $K = K_{max}$ remains unchanged.

The state at $K_{min} = 0$ may thus be analyzed in terms of the boundary-value problem illustrated in Fig. 5. We seek the elastic field (symmetrical about the x-axis) consistent with the conditions shown along the x-axis: a dislocation $\delta = \delta_R$ along $(-\infty, 0)$; $\sigma_y = -\sigma_Y$, the compressive yield stress, in $(0, a)$; and the dislocation $\delta = \delta_M = \delta_0 g(x/w)$ in (a, w) Since $K_{min} = 0$, the stresses σ_{ij} must decay faster

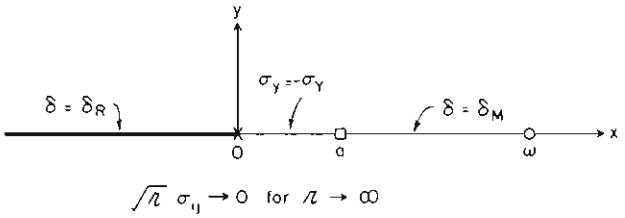

Fig. 5 Problem formulation, $K = K_{min} = 0$

than $r^{-1/2}$ for $r \to \infty$. Finally, we require that the stresses be bounded. This last condition, it will be seen, suffices to determine δ_R and a. It will also be shown that $|\sigma_y| \leq \sigma_Y$ everywhere along the x-axis and $\sigma_y \geq 0$ in the contact region.

An analysis involving the standard complex Mnskhelishvili potentials $\phi(z)$ and $\psi(z)$ may be used. Stress continuity across the x-axis permits the elimination of ψ [11], allowing the stresses to be written just in terms of ϕ as

$$\sigma_x + \sigma_y = 2[\phi'(z) + \bar{\phi}'(\bar{z})] \tag{7}$$

$$\sigma_y - i\tau_{xy} = \phi'(z) + \phi'(\bar{z}) + (z - \bar{z})\bar{\phi}''(\bar{z}) \tag{8}$$

The potential $\phi(z)$ must be everywhere analytic, except for a branch cut along $(-\infty, w)$ on the real axis. Along the x-axis, $\tau_{xy} = 0$, and so (8) gives, for z real,

$$\sigma_y = \phi_+' + \phi_-' \tag{9}$$

where

$$f_\pm \equiv f(x \pm i\eta) \qquad \eta > 0, \eta \to 0 \tag{10}$$

In plane stress, the displacements u and v in the x and y-directions satisfy

$$E\frac{\partial}{\partial x}(u + iv) = (3 - \nu)\phi'(z) - (1 + \nu)[\phi'(\bar{z}) + (z - \bar{z})\bar{\phi}''(\bar{z})] \tag{11}$$

Use of the continuity of u across the x-axis then leads to the result

$$\left(\frac{\partial v}{\partial x}\right)_+ - \left(\frac{\partial v}{\partial x}\right)_- = \frac{4}{iE}[\phi_+' - \phi_-'] \tag{12}$$

for the jump in $\partial v/\partial x$ across the x-axis. It follows from (9) and (12) that the following conditions on $\Phi \equiv \phi'$ must hold along the x-axis (see Fig. 5):

$$\left.\begin{aligned} &\Phi_+ - \Phi_- = 0 && \text{for} \quad x < 0 \\ &\Phi_+ + \Phi_- = -\sigma_Y && 0 < x < a \\ &\Phi_+ - \Phi_- = \frac{iE}{4}\frac{d\delta_M}{dx} && a < x < w \\ &\Phi_+ - \Phi_- = 0 && x > w \end{aligned}\right\} \tag{13}$$

With the introduction of $\chi \equiv \sqrt{z(z-a)}$ (branch cut on the interval $(0, a)$; $\chi \sim z$ for $|z| \to \infty$) equations (13) become equivalent to

$$\left.\begin{aligned} (\chi\Phi)_+ - (\chi\Phi)_- &= 0 && \text{for} \quad x < 0 \\ &= -\chi_+\sigma_Y && 0 < x < a \\ &= \frac{iE\chi}{4}\frac{d\delta_M}{dx} && a < x < w \\ &= 0 && x > w \end{aligned}\right\} \tag{14}$$

The general solution for $\chi\Phi$ then follows from a standard application of Plemelj integrals [11] as

$$\sqrt{z(z-a)}\Phi(z) = -\frac{\sigma_Y}{2\pi}\int_0^a \frac{\sqrt{x(a-x)}}{x - z}dx + \frac{E}{8\pi}\int_a^w \frac{\sqrt{x(x-a)}}{x - z}\frac{d\delta_M}{dx}dx + C \tag{15}$$

But the constant C can be immediately identified by use of the requirement that for $|z| \to \infty$, $\Phi(z)$ must be asymptotically equivalent to the potential corresponding to a dislocation δ_R all along the negative x-axis. This gives

$$C = \frac{E\delta_R}{8\pi} \tag{16}$$

It is convenient to introduce the nondimensional variables

$$\zeta = z/w, \quad \xi = x/w, \quad \alpha = a/w, \quad F = \left(\frac{\pi^2}{\sigma_Y}\right)\Phi \tag{17}$$

With the use of (3), the general eqnations (9) and (12) relating stresses and dislocations along the real axis to the stress function transform to

$$F_+ + F_- = \pi^2(\sigma_y/\sigma_Y) \tag{18}$$

and

$$F_+ - F_- = 2\pi i\frac{d}{d\xi}(\delta/\delta_0) \tag{19}$$

The result (15) becomes

$$\sqrt{\zeta(\zeta-\alpha)}F = -\frac{\pi^2}{2}[\sqrt{\zeta(\zeta-\alpha)} - \zeta + \alpha/2] + \frac{\delta_R}{\delta_0} + \int_\alpha^1 \frac{\sqrt{\xi(\xi-\alpha)}}{\xi - \zeta}\frac{d}{d\xi}\left(\frac{\delta_M}{\delta_0}\right)d\xi \tag{20}$$

wherein use has been made of

$$\int_0^\alpha \frac{\sqrt{\xi(\alpha-\xi)}}{\xi - \zeta}d\xi = \pi[\sqrt{\zeta(\zeta-\alpha)} - \zeta + \alpha/2]$$

for ζ not on the real axis in $(0, \alpha)$. We now assert, via (18), the boundedness of the stresses σ_y at $\zeta = 0, \alpha$; this gives the equations

$$\frac{\delta_R}{\delta_0} = \frac{\pi^2\alpha}{4} + \int_\alpha^1 \sqrt{\frac{\xi - \alpha}{\xi}}f_1(\xi)d\xi \tag{21}$$

$$\frac{\delta_R}{\delta_0} = -\frac{\pi^2\alpha}{4} + \int_\alpha^1 \sqrt{\frac{\xi}{\xi - \alpha}}f_1(\xi)d\xi \tag{22}$$

wherein we have introduced $\delta_M/\delta_0 = g(\xi)$ (see (4)) and

$$f_1(\xi) = -g'(\xi) = \frac{1}{2}\log\left|\frac{1 + \sqrt{1-\xi}}{1 - \sqrt{1-\xi}}\right| \tag{23}$$

Equations (21) and (22) combine to give

$$\frac{\pi^2}{2} = \int_\alpha^1 \frac{f_1(\xi)d\xi}{\sqrt{\xi(\xi-\alpha)}} \tag{24}$$

Solving (24) numerically for α gives

$$\alpha = 0.09286 \tag{25}$$

and then (21) gives the residual stretch as

$$\frac{\delta_R}{\delta_0} = 0.8562 \tag{26}$$

Thus, in contrast to the stationary crack, which suffers reverse plastic flow in an interval of size $w/4$, the growing fatigue crack has, in each cycle, reverse yielding in less than 10 percent of the Dugdale zone; and the residual stretch is a somewhat surprising 86 percent of the crack-tip stretch. For this solution at $K = 0$ to be valid, it is necessary that the contact stresses in $(-\infty, 0)$ along the x-axis satisfy $0 \geq \sigma_y \geq -\sigma_Y$. We find from (15) and (20) that for $\xi = x/w$ in $(-\infty, 0)$

$$\frac{\sigma_y}{\sigma_Y} = -1 + \sqrt{\frac{|\xi|}{\alpha + |\xi|}}\left[1 - \frac{2}{\pi^2}\int_\alpha^1 \frac{f_1(\tau)}{\tau + |\xi|}\sqrt{\frac{\tau - \alpha}{\tau}}d\tau\right]$$

and, it is found numerically, this gives a σ_y that varies monotonically from $-\sigma_Y$ at $\xi = 0$ to zero at $\xi = -\infty$. It can also be checked that $|\sigma_y| \leq \sigma_Y$ for $\xi \geq \alpha$ along the positive real axis.

Having determined the magnitude of the residual stretch, it is now possible for us to study the unloading and reloading processes in detail. If there were no residual stretch, the crack opening displacement

along $x < 0$ as a function of K, as K *decreases* from K_{max}, would be

$$\delta/\delta_0 = g(x/w) - (2a_K/w)g(x/a_K) \tag{27}$$

where a_K given by

$$a_K = \frac{w}{4}\left(1 - \frac{K}{K_{max}}\right)^2 \tag{28}$$

is the varying size of the reverse plastic yield zone during the unloading process. This result follows simply from the superposition on the displacements (4) of a similar, scaled displacement associated with a yield stress of $(-2\sigma_Y)$ in a zone of length a_K given by (see (2))

$$a_K = \frac{\pi}{8}\left(\frac{K_{max} - K}{2\sigma_Y}\right)^2.$$

We note that (27) has a local minimum in $(-\infty, 0)$, so that when the stretch $\delta_R/2$ is attached to each crack face, the first contact will occur at values of x and a_K that satisfy

$$g(x/w) - 2(a_K/w)g(x/a_K) = \delta_R/\delta_0 \tag{29}$$

and

$$g'(x/w) - 2g'(x/a_K) = 0 \tag{30}$$

Denote the critical values of (x/w) and (a_K/w) by ξ_c and α_c, respectively; then

$$\left.\begin{aligned} g(\xi_c) - 2\alpha_c g(\xi_c/\alpha_c) &= \delta_R/\delta_0 \\ -f_1(\xi_c) + 2f_1(\xi_c/\alpha_c) &= 0 \end{aligned}\right\} \tag{31}$$

where

$$\alpha_c = \frac{1}{4}\left(1 - \frac{K_{cont}}{K_{max}}\right)^2 \tag{32}$$

in terms of the nominal stress intensity factor K_{cont} at contact. It turns out, with the help of the fact that $g(\xi) = \sqrt{1-\xi} - \xi f_1(\xi)$, that (31) can be solved analytically, with the results

$$\alpha_c = \frac{1 - (\delta_R/\delta_0)^2}{4} \tag{33}$$

and

$$\xi_c = -\frac{4\alpha_c^2}{1 - 4\alpha_c} = -\frac{[1 - (\delta_R/\delta_0)^2]^2}{4(\delta_R/\delta_0)^2} \tag{34}$$

Then (32) gives

$$\frac{K_{cont}}{K_{max}} = 1 - \sqrt{1 - (\delta_R/\delta_0)^2} \tag{35}$$

With (26), these give

$$\alpha_c = 0.0667, \quad \xi_c = -0.0243, \quad \frac{K_{cont}}{K_{max}} = 0.483 \tag{36}$$

Thus first contact occurs very close to the crack tip. With the residual stretch taken into account, the net crack-tip opening displacement $(\delta_{Tc} - \delta_R)$ at contact is given by (see (27))

$$\frac{\delta_{Tc} - \delta_R}{\delta_0} = 1 - 2\alpha_c - \frac{\delta_R}{\delta_0} = 0.010 \tag{37}$$

which is very small indeed.

As the load is reduced further from K_{cont} the boundaries of the finite contact zone will move to opposite sides of the initial point of contact, with complete closure along $x \leq 0$ eventually occurring at $K = 0$. We shall not analyze this process in detail (although there is no essential difficulty in doing so) and consider next the process of reloading from $K = 0$. It turns out that the contact region starts to open at $-\infty$, with the edge of the contact zone at $x = b$ $(b < 0)$ moving in toward the crack tip as K increases, and during the reloading process closure is maintained between $x = b$ and the crack tip. As long as there is any amount of crack closure, the stress changes remain elastic, and the formulation of the appropriate elastic problem is illustrated in

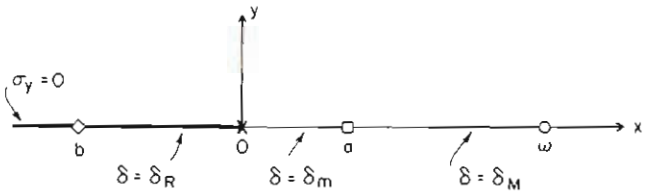

$$\sigma_{ij} \sim K\sigma_{ij}^0 \quad \text{for } r \to \infty$$

Fig. 6 Problem formulation, K increasing, $K < K_{open}$

Fig. 6 for $-\infty < b \leq 0$. In this figure, the dislocation $\delta = \delta_m$ in the interval $(0, a)$ represents the plastic stretch left over from the state at $K = K_{min} = 0$. From (19) and (20), with the use of (21) and (24), we find in $(0, \alpha)$

$$\frac{d}{d\xi}\left(\frac{\delta_m}{\delta_0}\right) \equiv -f_2(\xi) = -\frac{1}{\pi}\sqrt{\xi(\alpha - \xi)}\int_\alpha^1 \frac{f_1(\tau)d\tau}{(\tau - \xi)\sqrt{\tau(\tau - \alpha)}} \tag{38}$$

(It can be verified that this gives

$$\lim_{\xi \to \alpha} f_2(\xi) = f_1(\alpha).$$

as it should.) The problem illustrated in Fig. 6 can now be formulated directly in the ζ-plane, in terms of a new $F(\zeta)$. Accordingly, with $\xi = x/w$ and $\beta = b/w$, we want

$$\left.\begin{aligned} F_+ + F_- &= 0 && \text{for} \quad \xi < \beta \\ F_+ - F_- &= 0 && \beta < \xi < 0 \\ F_+ - F_- &= 2\pi i \frac{d}{d\xi}(\delta_m/\delta_0) && 0 < \xi < \alpha \\ F_+ - F_- &= 2\pi i \frac{d}{d\xi}(\delta_M/\delta_0) && \alpha < \xi < 1 \\ &= 0 && \xi > 1 \end{aligned}\right\} \tag{39}$$

Also, the potential Φ associated with the stresses (1) is

$$\Phi = \frac{K}{2\sqrt{2\pi z}}$$

so that the far-field behavior of F is

$$F \sim \frac{\pi}{\sqrt{\zeta}}\frac{K}{K_{max}} \tag{40}$$

Introducing

$$\psi(\zeta) = \sqrt{\zeta - \beta} \quad \text{(branch line along } \xi < \beta\text{; } \psi(1) = +\sqrt{1-\beta})$$

permits the conditions (39) to be transformed to

$$\left.\begin{aligned} (\psi F)_+ - (\psi F)_- &= 0 && \text{for} \quad \xi < 0 \\ &= 2\pi i \psi \frac{d}{d\xi}(\delta_m/\delta_0) && 0 < \xi < \alpha \\ &= 2\pi i \psi \frac{d}{d\xi}(\delta_M/\delta_0) && \alpha < \xi < 1 \\ &= 0 && \xi > 1 \end{aligned}\right\}$$

Then the Plemelj integral solution satisfying (40) becomes

$$\sqrt{\zeta - \beta}F(\zeta) = \int_0^\alpha \frac{\sqrt{\xi - \beta}}{\xi - \zeta}\frac{d}{d\xi}\left(\frac{\delta_m}{\delta_0}\right)d\xi + \int_\alpha^1 \frac{\sqrt{\xi - \beta}}{\xi - \zeta}\frac{d}{d\xi}\left(\frac{\delta_M}{\delta_0}\right)d\xi + \pi\frac{K}{K_{max}} \tag{41}$$

for the reloading process, with $\beta \leq 0$.

To keep σ_y bounded at $\zeta = \beta$ we require

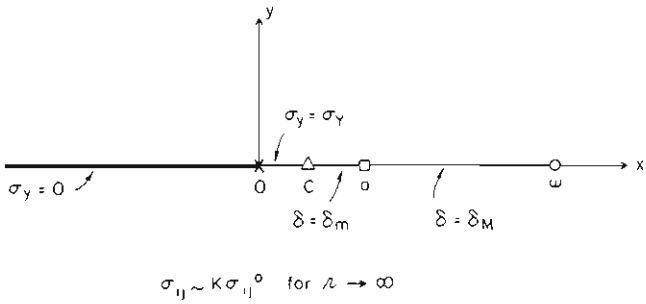

Fig. 7 Problem formulation, K increasing, $K > K_{open}$

$$\frac{K}{K_{max}} = \frac{1}{\pi}\int_0^{\alpha} \frac{f_2(\xi)d\xi}{\sqrt{\xi-\beta}} + \frac{1}{\pi}\int_{\alpha}^{1} \frac{f_1(\xi)d\xi}{\sqrt{\xi-\beta}} \tag{42}$$

Here $f_2(\xi)$ must be calculated numerically from (38). By picking values of $\beta < 0$, we can calculate directly from (42) the variation of K with the position of boundary b of the contact region as the crack is opened up. Of most interest, however, is the value K_{open} of the nominal stress-intensity factor associated with $b = 0$, when the crack has finally been fully opened up, and the region ahead of the crack is on the verge of yielding in tension again. Thus, if we set $\beta = 0$ in (42), we get

$$\frac{K_{open}}{K_{max}} = \frac{1}{\pi}\int_0^{\alpha} \frac{f_2(\xi)d\xi}{\sqrt{\xi}} + \frac{1}{\pi}\int_{\alpha}^{1} \frac{f_1(\xi)d\xi}{\sqrt{\xi}} \tag{43}$$

which, by numerical integration, gives

$$K_{open}/K_{max} = 0.557 \tag{44}$$

Continued reloading beyond K_{open} will produce plastic restretching in an interval $(0, c)$ where $c < a$. The problem formulation is sketched in Fig. 7, and, with $\gamma = c/w$, and $\psi = \sqrt{\zeta - \gamma}$, the conditions on $F(\zeta)$ become

$$\left.\begin{aligned}
(\psi F)_+ - (\psi F)_- &= 0 && \text{for} \quad \xi < 0 \\
&= \pi^2\psi_+ && 0 < \xi < \gamma \\
&= 2\pi i\psi \frac{d}{d\xi}(\delta_m/\delta_0) && \gamma < \xi < \alpha \\
&= 2\pi i\psi \frac{d}{d\xi}(\delta_M/\delta_0) && \alpha < \xi < 1 \\
&= 0 && \xi > 1
\end{aligned}\right\} \tag{45}$$

The solution is

$$\sqrt{\zeta-\gamma}F = \frac{\pi}{2}\int_0^{\gamma} \frac{\sqrt{\gamma-\xi}}{\xi-\zeta}d\xi + \int_{\gamma}^{\alpha} \frac{\sqrt{\xi-\gamma}}{\xi-\zeta}\frac{d}{d\xi}\left(\frac{\delta_m}{\delta_0}\right)d\xi + \int_{\alpha}^{1} \frac{\sqrt{\xi-\gamma}}{\xi-\zeta}\frac{d}{d\xi}\left(\frac{\delta_M}{\delta_0}\right)d\xi + \pi\frac{K}{K_{max}} \tag{46}$$

Requiring bounded behavior at $\zeta = \gamma$ then gives

$$\frac{K}{K_{max}} = \sqrt{\gamma} + \frac{1}{\pi}\int_{\gamma}^{\alpha} \frac{f_2(\xi)d\xi}{\sqrt{\xi-\gamma}} + \frac{1}{\pi}\int_{\alpha}^{1} \frac{f_1(\xi)d\xi}{\sqrt{\xi-\gamma}} \tag{47}$$

as the relation between the size $\gamma = (c/w)$ of the restretched region, and $K > K_{open}$. For $\gamma = 0$, we recover the result (43) for K_{open}/K_{max}. It can be shown that

$$\frac{1}{\pi}\int_{\alpha}^{1} \frac{f_1(\xi)d\xi}{\sqrt{\xi-\alpha}} = 1 - \sqrt{\alpha} \tag{48}$$

for $0 \le \alpha \le 1$, so that $K/K_{max} \to 1$ for $\gamma \to \alpha$. Also, it follows that an expression for K/K_{max} equivalent to (47) is

$$\frac{K}{K_{max}} = 1 - \frac{1}{\pi}\int_{\gamma}^{\alpha} \frac{f_1(\xi) - f_2(\xi)}{\sqrt{\xi-\gamma}}d\xi \tag{49}$$

and so we also have

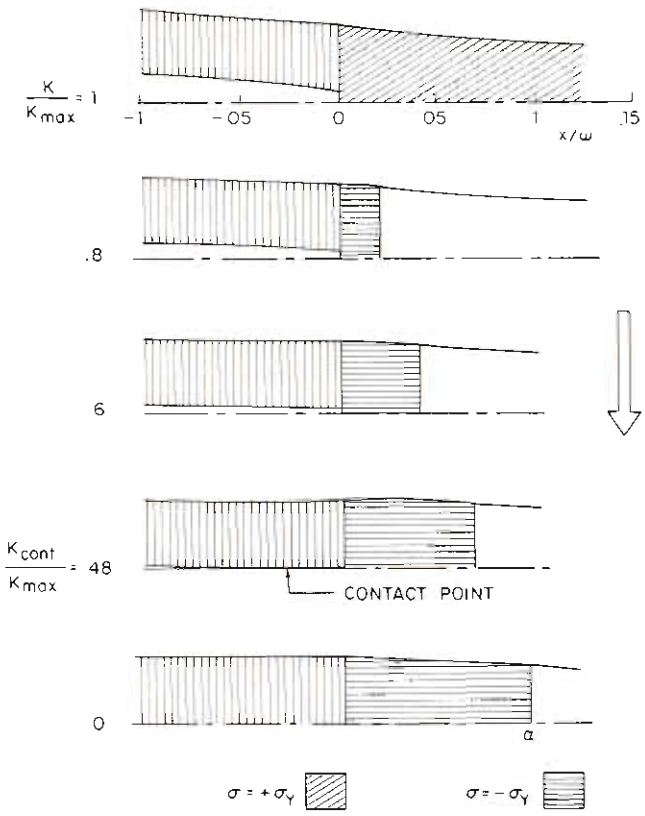

Fig. 8(*a*) Crack closing process ($K = K_{max} \to K = 0$)

$$\frac{K_{open}}{K_{max}} = 1 - \frac{1}{\pi}\int_0^{\alpha} \frac{f_1(\xi) - f_2(\xi)}{\sqrt{\xi}}d\xi \tag{50}$$

For any value of β in $(-\infty, 0)$, or γ in $(0, \alpha)$ and the corresponding values of K/K_{max}, dislocations δ/δ_0 can be calculated wherever they were unspecified. For example, for $\gamma > 0$ and $\xi < \gamma$, use of (46) in (39) and subsequent iuntegration leads eventually (we omit details) to

$$\frac{\delta}{\delta_0} = -2\sqrt{\gamma-\xi}\left(1 - \frac{K}{K_{max}}\right) + g(\xi) - \frac{2}{\pi}\int_{\gamma}^{\alpha} [f_1(\tau) - f_2(\tau)] \arctan\sqrt{\frac{\tau-\gamma}{\gamma-\xi}}d\tau \tag{51}$$

For $0 \le \xi \le \gamma$, this gives the plastic stretch during reloading past K^*_{open}; and for $\xi \le 0$, $(\delta/\delta_0 - \delta_R/\delta_0)$ provides the crack-opening displacement left after the residual stretch is suhtracted off. This formula, together with equations (27) and (28) for δ/δ_0 during the unloading phase down to $K = K_{cont}$, were used to prepare the scaled diagrams of Figs. 8(a and b), which show what happens during one cycle of unloading from K_{max} to $K = 0$, and then reloading back to K_{max}. Fig. 8(a) illustrates the spread of the reverse yielding zone as K decreases, and shows, at $K \approx 0.48$, how very close to crack-tip closure is the situation when first contact occurs just to the left of the tip. In view of the idealized assumptions of the present analysis it would evidently be absurd to try to corroborate experimentally the precise location of the initial contact poiut. In Fig. 8(b) we skip over the details of the behavior between $K = 0$ and K_{open}, during which the edge of the contact region sweeps in toward the crack tip. For K increasing above K_{open}, the sketches show how the zone of plastic reloading spreads into the region ahead of the crack tip until the initial configuration reasserts itself at $K = K_{max}$. Note that in the region $a/w < x < 1$, the yield stress σ_Y in tension is just barely reattained, with no additional stretch occurring.

In Fig. 9, we show how the crack-tip plastic stretch varies with K/K_{max} during one cycle of loading. The rising part of the curve, for

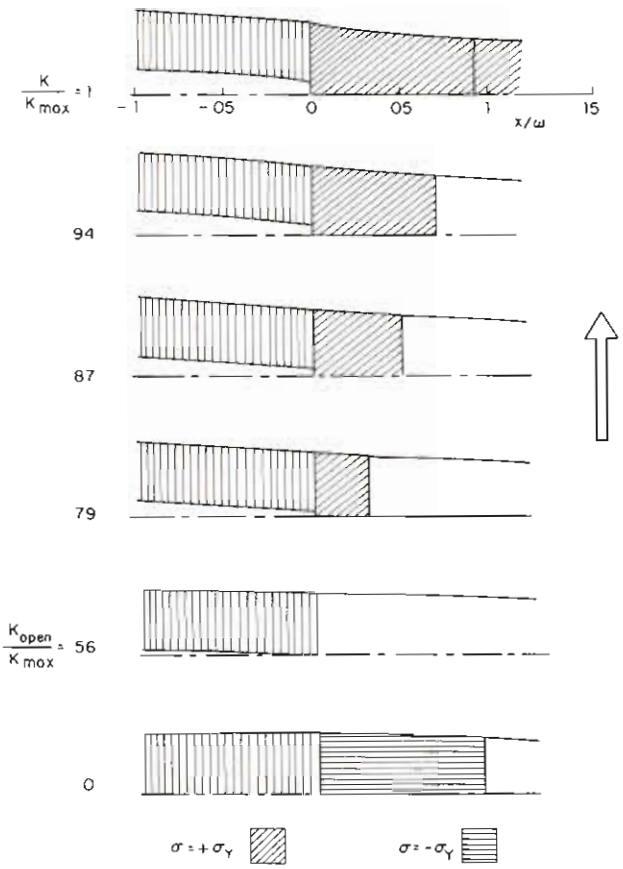

Fig. 8(*b*) Crack opening process ($K = 0 \rightarrow K = K_{max}$)

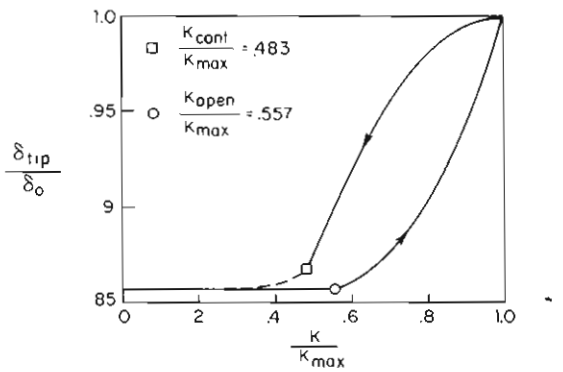

Fig. 9 Crack-tip stretch versus K/K_{max}

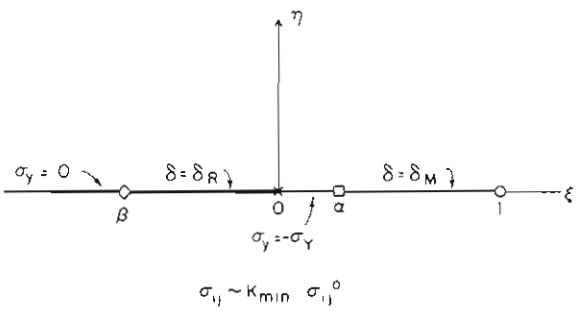

Fig. 10 Problem formulation, $K = K_{min} > 0$

to apply to the vicinity of a moving crack tip in the following sense: Let Δ be the crack growth per cycle; then we have really addressed the problem for the asymptotic limit $\Delta/w \rightarrow 0$.

Growing Crack ($K_{min} > 0$). For a positive value of the load ratio $R = K_{min}/K_{max}$, a similar analysis can be executed. The situation for $K = K_{min}$, in particular the magnitude of the residual stretch δ_R and the reverse plastic zone length $a = \alpha w$, can be determined on the basis of the conditions indicated in Fig. 10, this time directly in the ζ-plane. For $K_{min} > 0$, it is to be expected that the contact will terminate at $x = b = \beta w$ ($\beta < 0$). The conditions on F are

$$\left.\begin{aligned} F_+ + F_- &= 0 && \text{for} \quad \xi < \beta \\ F_+ - F_- &= 0 && \beta < \xi < 0 \\ F_+ + F_- &= -\pi^2 && 0 < \xi < \alpha \\ F_+ - F_- &= 2\pi i \frac{d}{d\xi}(\delta_M/\delta_0) && \alpha < \xi < 1 \\ F_+ - F_- &= 0 && \xi > 1 \end{aligned}\right\} \tag{53}$$

We now introduce the auxiliary function

$$\psi = \sqrt{(\zeta - \beta)(\zeta)(\zeta - \alpha)} \text{ (branch lines along } (-\infty, \beta) \text{ and } (0, \alpha);$$
$$\psi(1) = +\sqrt{(1 - \beta)(1 - \alpha)}) \tag{54}$$

and then

$$\left.\begin{aligned} (\psi F)_+ - (\psi F)_- &= 0 && \text{for} \quad \xi < 0 \\ &= -\pi^2 \psi_+ && 0 < \xi < \alpha \\ &= 2\pi i \psi \frac{d}{d\xi}(\delta_M/\delta_0) && \alpha < \xi < 1 \\ &= 0 && \xi > 1 \end{aligned}\right\} \tag{55}$$

For $\zeta \rightarrow \infty$, we want $F \sim \pi(K_{min}/K_{max})/\sqrt{\zeta}$, so that

$$\sqrt{(\zeta - \beta)(\zeta)(\zeta - \alpha)}F(\zeta) = -\frac{\pi}{2}\int_0^\alpha \frac{\sqrt{(\xi - \beta)(\xi)(\alpha - \xi)}}{\xi - \zeta} d\xi + \int_\alpha^1 \frac{\sqrt{(\xi - \beta)(\xi)(\xi - \alpha)}}{\xi - \zeta} \frac{d}{d\xi}\left(\frac{\delta_M}{\delta_0}\right) d\xi + \pi[A + (K_{min}/K_{max})\zeta] \tag{56}$$

$K > K_{open}$ is given by equation (51), with $\xi = 0$; from (27) and (28), the deseending curve, down to K_{cont}, is just

$$\delta_{tip}/\delta_0 = 1 - \frac{1}{2}(1 - K/K_{max})^2 \tag{52}$$

The variation on the unloading curve between K_{cont} and $K = 0$ was not calculated, but must follow a path like the interpolated dashed line.

Although all of the foregoing analysis and discussion comes under the heading "Growing Crack," we have not given explicit consideration to the actual process of crack extension, which is imagined to occur in a small step at any time during the cycle of loading and unloading. The stress and deformation analysis we have given may be considered

where A is a constant to be determined. Indeed, making the Cauchy principal value of the right-hand side of (56) vanish at $\zeta = \beta$, 0, and α provides three relations among the quantities K_{min}/K_{max}, α, β, and A. For various assumed values of α between 0.09286 (corresponding to $K_{min} = 0$) and $\alpha = 0$, it was relatively straightforward to solve these equations (we omit details again) for K_{min}, β, and A. To determine the associated value of δ_R/δ_0, we used these values in (56) and (19) to calculate $(d/d\xi)(\delta/\delta_0)$ numerically in $(0, \alpha)$ (with $(d/d\xi)(\delta/\delta_0) = 0$ and $-f_1(\alpha)$ at the endpoints of the interval). Finally, we found

$$\delta_R/\delta_0 = g_1(\alpha) - \int_0^\alpha \frac{d}{d\xi}\left(\frac{\delta}{\delta_0}\right) d\xi$$

The results of these calculations are summarized in Fig. 11, which

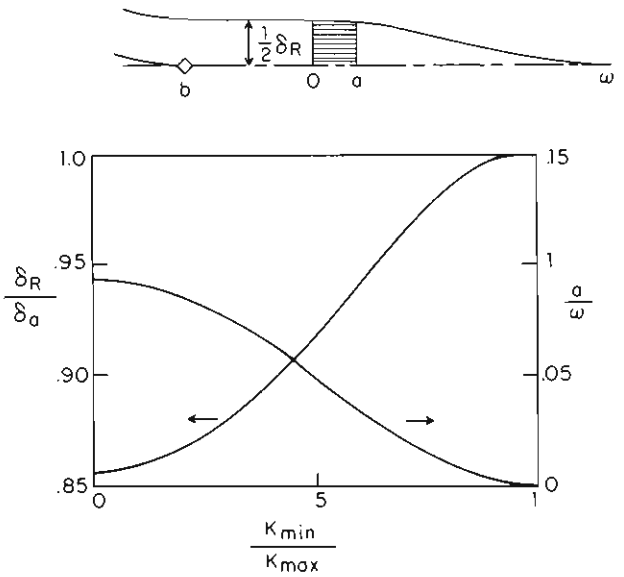

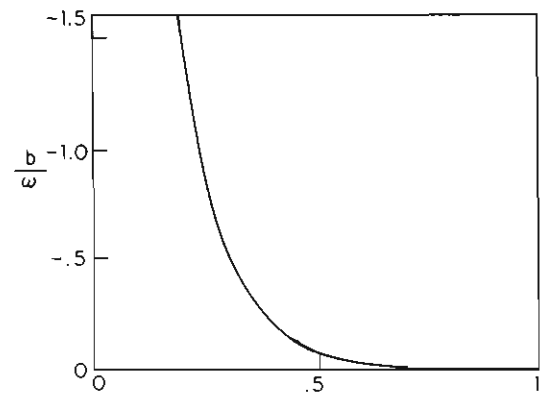

Fig. 11 Residual stretch, lift-off point, and compressive yield zone at $K = K_{min}$

shows plots of δ_R/δ_0, a/w, and b/w at $K = K_{min}$ as functions of K_{min}/K_{max}.

The value of K at first contact during the unloading process can now be found directly form equation (35), which remains applicable at all values of K_{min}/K_{max} between zero and unity. Furthermore, the opening loads are still given by equation (43) with the understanding that, for a given value of α, $f_2(\xi) = -d(\delta_m/\delta_0)/d\xi$ now refers to the residual stretch in $(0, \alpha)$ already found earlier for the calculation of δ_R/δ_{max}, and the results apply to the value of K_{min}/K_{max} associated with the given value of α. The results for both K_{cont}/K_{max} and K_{open}/K_{max} are shown as functions of K_{min}/K_{max} in Fig. 12. We remark that both curves are quite close to Elber's experimentally estimated formula

$$K_{open}/K_{max} \approx 0.5 + 0.1(K_{min}/K_{max}) + 0.4(K_{min}/K_{max})^2$$

However, not all experimental data collected to date substantiate this formula (e.g., [9]).

We do not address, in this paper, the question of predicting the crack-growth-rate per cycle. However, the present results do provide a theoretical basis for the use of a closure-based effective stress-intensity range $(\Delta K)_{eff}$ in correlating crack-growth rates for different load ratios K_{min}/K_{max}. By cross-plotting the results of Figs. 11 and 12, we find that the cyclic stretch at the crack tip is fairly well approximated by (Fig. 13(*a*))

$$\frac{\delta_0 - \delta_R}{\delta_0} \approx 0.73 \left(\frac{K_{max} - K_{open}}{K_{max}}\right)^2 \tag{57}$$

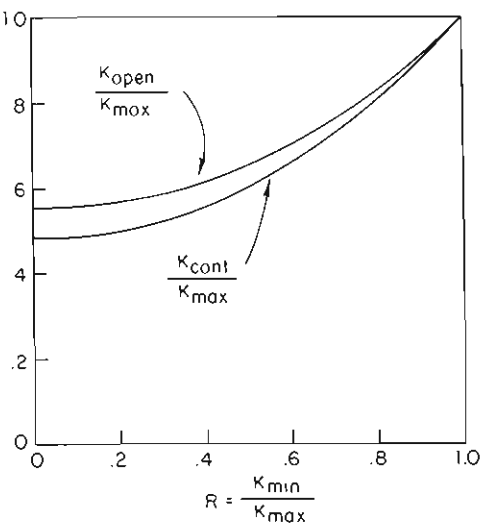

Fig. 12 Opening and contact load ratios versus K_{min}/K_{max}

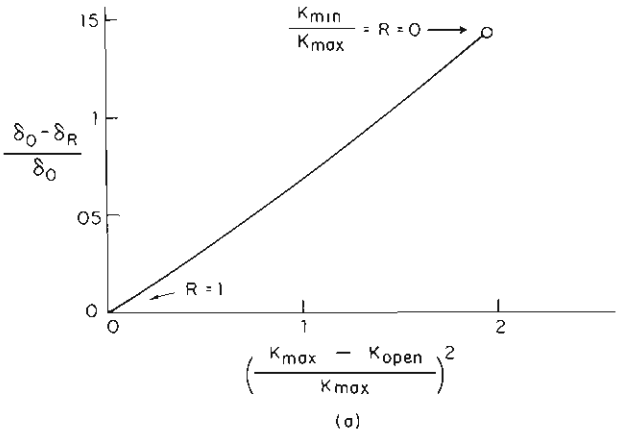

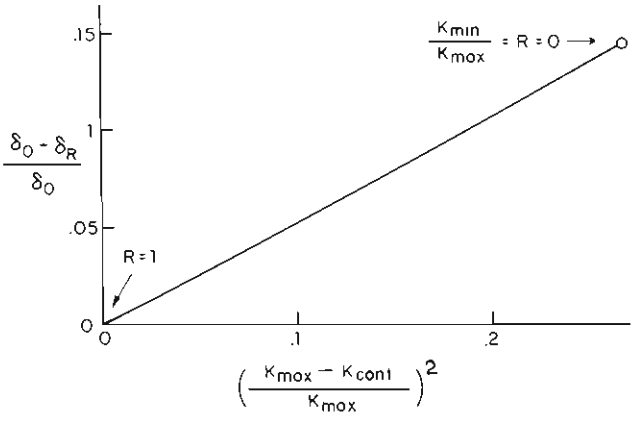

Fig. 13 Cyclic-stretch ratio (*a*) $\Delta K_{eff} \sim (K_{max} - K_{open})$ and (*b*) $\Delta K_{eff} \sim (K_{max} - K_{cont})$

or by (Fig. 13(*b*))

$$\frac{\delta_0 - \delta_R}{\delta_0} \approx 0.54 \left(\frac{K_{max} - K_{cont}}{K_{max}}\right)^2 \tag{58}$$

By equation (3), these are the same as

$$\delta_0 - \delta_R \approx 0.73(K_{max} - K_{open})^2/(E\sigma_Y) \tag{59}$$

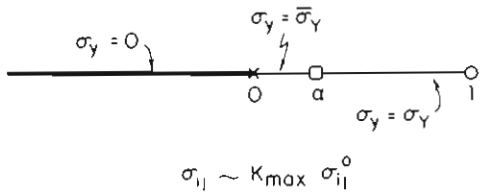

Fig. 14 Problem formulation, cyclic hardening, $K = K_{max}$

and

$$\delta_0 - \delta_R \approx 0.54(K_{max} - K_{cont})^2/(E\sigma_Y) \tag{60}$$

The point of these observations is that the craek-growth rate for a particular material ought to he a function of the cyclic-stretch $\delta_0 - \delta_R$. Hence the approximate validity of (59) and (60) suggests that crack-growth-rate might equally well he a function of an effective stress-intensity range defined by either $(\Delta K)_{eff} = K_{max} - K_{open}$ or $(\Delta K)_{eff} = K_{max} - K_{coat}$, independently—at least as a first approximation—of K_{min}/K_{max}. Experimental evidence on this hypothesis is inconclusive, with indications [12] that K_{max}/K_c is another significant parameter when it is not too small, where K_c is the critical stress intensity for static failure.

Effects of Cyclic Hardening. The calculations made so far can readily be modified to incorporate the effects of a presumed change in the yield stress in the region ahead of the crack tip that undergoes repeated reverse plastic flow. We continue to denote the original yield stresses by $\pm\sigma_Y$ but let the hardened (or softened) ones be $\pm\bar{\sigma}_Y$ in tension and compression. We will present abbreviated descriptions of the modifications that arise when cyclic hardening is taken into account.

At $K = K_{max}$, a modified Dugdale solution for F must satisfy the conditions shown in Fig. 14. The size of the plastic zone is still denoted by w. The relative size $\alpha = a/w$ of the reverse yielding zone is, of course, as yet unknown, but it coiucides with the interval withiu which the yield stress must be taken as $\bar{\sigma}_Y$ rather than σ_Y. It is readily found that, with $s = \bar{\sigma}_Y/\sigma_Y$,

$$\sqrt{\zeta - 1}F = \frac{\pi s}{2}\int_0^\alpha \frac{\sqrt{1-\xi}}{\xi - \zeta}\,d\xi + \frac{\pi}{2}\int_\alpha^1 \frac{\sqrt{1-\xi}}{\xi - \zeta}\,d\xi + \pi\frac{K_{max}}{K_0} \tag{61}$$

where we have introduced the reference stress intensity

$$K_0 = 2\sigma_Y\sqrt{2w/\pi} \tag{62}$$

This (see (2)) is the stress intensity that would correspond to the plastic zone size w if $\bar{\sigma}_Y$ were the same as σ_Y. Requiring bounded stress at $\xi = 1$ then gives

$$K_{max}/K_0 = s - (s-1)\sqrt{1-\alpha} \tag{63}$$

The dislocations implied by (61) for $\xi \leqq 1$ are found to satisfy

$$\frac{d}{d\xi}\left(\frac{\delta}{\delta_0}\right) \equiv -\bar{f}_1(\xi, \alpha, s) = -[sf_1(\xi) - (s-1)q(\xi, \alpha)] \tag{64}$$

where

$$q(\xi, \alpha) = \frac{1}{2}\log\left|\frac{\sqrt{1-\alpha} + \sqrt{1-\xi}}{\sqrt{1-\alpha} - \sqrt{1-\xi}}\right| \tag{65}$$

and we have used $\delta_0 = 8\sigma_Y w/(\pi E)$, the tip stretch for $s = 1$, as a normaliziug quantity. (Note that δ_0 is *not* the crack-tip stretch for $s \neq 1$.) Integration of (64) gives

$$\delta/\delta_0 = [s - (s-1)\sqrt{1-\alpha}]\sqrt{1-\xi} - s\xi f_1(\xi) + (s-1)(\xi - \alpha)q(\xi, \alpha)$$
$$\equiv \bar{g}(\xi, \alpha, s) \tag{66}$$

and so the actual crack-tip stretch, $(\delta_T)_{max}$, is given by

$$\frac{(\delta_T)_{max}}{\delta_0} = \frac{K_{max}}{K_0} - (s-1)\left(\frac{\alpha}{2}\right)\log\left|\frac{1+\sqrt{1-\alpha}}{1-\sqrt{1-\alpha}}\right| \tag{67}$$

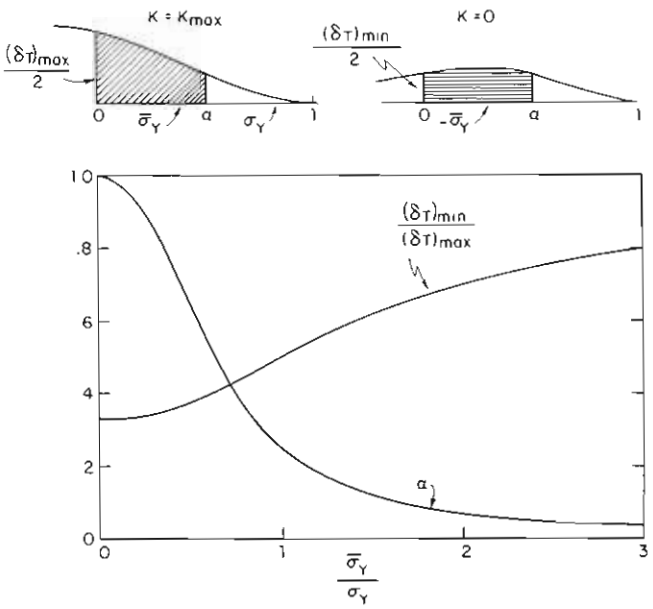

Fig. 15 Effect of cyclic hardening or softening—stationary crack with no closure

(Note that $\bar{f}_1(\xi, \alpha, 1) = f_1(\xi)$, and $\bar{g}(\xi, \alpha, 1) = g(\xi)$.)

It may be instructive to look first at the cyclic loading of a *stationary* crack, in which cyclic hardening or softening occurs in the reverse yielding region $(0, \alpha)$, but no residual stretches have been attached to the crack faces, and no closure effects occur. It is easy to see that after unloading, the dislocations at $K = K_{min}$ are given by

$$\delta/\delta_0 = \bar{g}(\xi, \alpha, s) - 2s\alpha g(\xi/\alpha) \tag{68}$$

where α is determined by

$$\alpha = \frac{1}{4s^2}\left(\frac{K_{max} - K_{min}}{K_0}\right)^2 \tag{69}$$

If we call the residual crack-tip stretch $(\delta_T)_{min}$, we have, from (63), (67), and (68)

$$\frac{(\delta_T)_{min}}{(\delta_T)_{max}} = 1 - 2s\alpha$$
$$\times\left\{s - (s-1)\left[\sqrt{1-\alpha} + \frac{\alpha}{2}\log\left|\frac{1+\sqrt{1-\alpha}}{1-\sqrt{1-\alpha}}\right|\right]\right\}^{-1} \tag{70}$$

From (63) and (69), we have

$$\frac{2s\sqrt{\alpha}}{[s - (s-1)\sqrt{1-\alpha}]} = 1 - \frac{K_{min}}{K_{max}} \tag{71}$$

For given values of K_{min}/K_{max} aud s, equations (70) and (71) provide the associated values of α and $(\delta_T)_{min}/(\delta_T)_{max}$. Fig. 15 shows such results for the case $K_{min}/K_{max} = 0$. We see that for $\bar{\sigma}_Y/\sigma_Y > 1$, $(\delta_T)_{min}/(\delta_T)_{max}$ increases from its value ½ for $\sigma_Y = \bar{\sigma}_Y$. Curiously, for cyclic softeuing, as $\bar{\sigma}_Y/\sigma_Y \to 0$, the stretch ratio approaches ⅓. These results for the stationary crack lead us to anticipate that the growing crack will suffer more severe crack-closure interference effects for $\bar{\sigma}_Y/\sigma_Y > 1$.

The analysis for the growing crack, with $K = K_{min} = 0$ will now be outlined. The problem setup is the same as that shown in Fig. 5 (in the z-plane) except that $\sigma_y = -\bar{\sigma}_Y$ in $(0, a)$. The solution for F retains the form of equation (20), except that the initial bracketed term gets multiplied by s, and $(d/d\xi)(\delta_M/\delta_0)$ in the iutegral is now defined by $-\bar{f}_1(\xi, \alpha, s)$ as given by (64). Similarly, equation (24) for the determination of α is replaced by

$$\frac{\pi^2 s}{2} = \int_\alpha^1 \frac{\bar{f}_1(\xi, \alpha, s)d\xi}{\sqrt{\xi(\xi - \alpha)}} \tag{72}$$

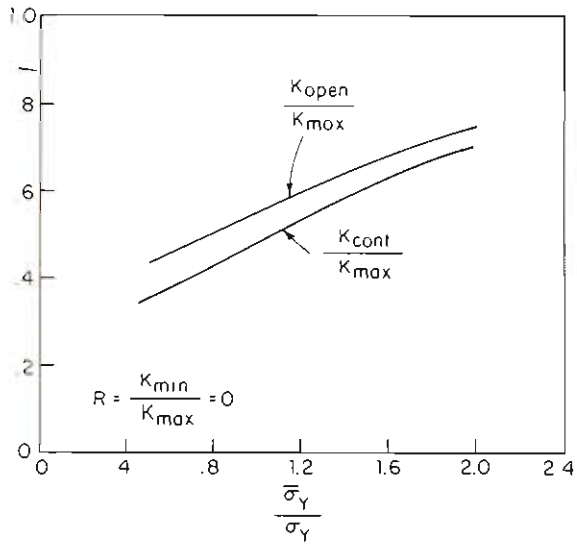

Fig. 16 Effect of cyclic hardening and softening on K_{cont} and K_{open}

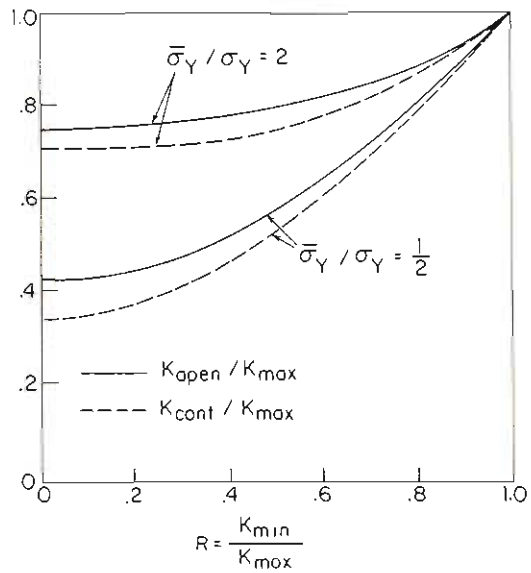

Fig. 17 Opening and contact load ratios versus K_{min}/K_{max} for cyclic hardening, $\bar{\sigma}_Y/\sigma_Y = 2$, and cyclic softening, $\bar{\sigma}_Y/\sigma_Y = 1/2$

Finally, δ_R/δ_0 becomes

$$\frac{\delta_R}{\delta_0} = \frac{\pi^2 s\alpha}{4} + \int_\alpha^1 \sqrt{\frac{\xi-\alpha}{\xi}}\,\bar{f}_1(\xi, \alpha, s)d\xi \tag{73}$$

The results for $K = K_{min} > 0$ also follow a pattern very similar to that for $s = 1$. In equation (56) for F, we simply multiply the first integral by s, use $(d/d\xi)(\delta_M/\delta_0) = -\bar{f}_1(\xi, \alpha, s)$, and replace K_{min}/K_{max} by K_{min}/K_0. With s assigned, the subsequent computation of K_{min}/K_0, A, and β for any assumed value of α proceeds as before. Since, for assumed s and α, K_{max}/K_0 is given by (63), the calculation of K_{min}/K_0 lets us find the load ratio K_{min}/K_{max}. To determine δ_R we use the modified F for $K = K_{min}$ to calculate $(d/d\xi)(\delta/\delta_0) \equiv -f_2(\xi)$ in $(0, \alpha)$, and then integrate to get

$$\frac{\delta_R}{\delta_0} = \frac{K_{max}}{K_0}\sqrt{1-\alpha} - s\alpha f_1(\alpha) + \int_0^\alpha f_2(\xi)d\xi$$

To compute K_{cont}, we must assert the appropriate modifications of equations (31) and (32), which are readily found to be (see the related equations (68) and (69))

$$\left.\begin{aligned} \bar{g}(\xi_c, \alpha, s) - 2s\alpha_c g(\xi_c/\alpha_c) &= \delta_R/\delta_0 \\ -\bar{f}_1(\xi_c, \alpha, s) + 2sf_1(\xi_c/\alpha_c) &= 0 \end{aligned}\right\} \tag{74}$$

and

$$\alpha_c = \frac{1}{4s^2}\left(\frac{K_{max} - K_{cont}}{K_0}\right)^2 \tag{75}$$

An analytic solution of (74) for $s \neq 1$ was not apparent, but for known values of α, s, and δ_R/δ_0, solutions for ξ_c and α_c may be found numerically. Then (75), together with (63) for K_{max}/K_0, gives K_{cont}/K_{max}.

The calculation of K_{open} is entirely straightforward, differing not at all in principle from that for $s = 1$. We simply use (43) as a formula for K_{open}/K_0, with $f_1(\xi)$ replaced by $\bar{f}_1(\xi, \alpha, s)$, and $f_2(\xi)$ still understood to be $-(d/d\xi)(\delta/\delta_0)$ *at* $K = K_{min}$. Again, K_{open}/K_{max} is then found with the use of (63).

Some numerical results obtained by these calculations are shown in Figs. 16 and 17. For $K_{min}/K_{max} = 0$, we show in Fig. 16 how K_{open}/K_{max} and K_{cont}/K_{max} vary with the cyclic hardening ratio $\bar{\sigma}_Y/\sigma_Y$. The trends are plausible and unsurprising. To complement Fig. 12, analogous results are shown in Fig. 17 for stress ratios $\bar{\sigma}_Y/\sigma_Y = 2$ and $1/2$.

Concluding Remarks

The analysis and results given in this paper lend theoretical support to the existence of the crack-closure phenomenon in fatigue crack-growth, elucidate the mechanics of this behavior, and provide some justification for the adoption of an effective stress-intensity range, based on closure effects, for the correlation of fatigue crack growth rates. Consideration of cyclic hardening effects show how such hardening produces increased closure effects, while cyclic softening alleviates them. On the other hand, the Dugdale model on which the analysis is based is not directly applicable to the plane strain conditions presumed to apply over most of the crack-tip region, and so a plane-strain analysis complementary to the present one would be welcome. Such an analysis would help to resolve the current uncertainty concerning the extent to which closure actually occurs under plane-strain conditions.

Acknowledgment

We are deeply indebted to Prof. James R. Rice, who gave us crucial advice in the initial stages of this work, and to Prof. Paul C. Paris, who encouraged us to study the problem. This work was started at the July 1976 meeting of the DARPA Materials Research Council, administered under Contract MDA-76-C-0250 by the University of Michigan, and received continuing financial support from the Air Force Office of Scientific Research under Grant AFOSR-77-3330 and the Division of Applied Sciences, Harvard University.

References

1 Elber, W., "Fatigue Crack Closure Under Cyclic Tension," *Engineering Fracture Mechanics*, Vol. 2, No. 1, July 1970, pp. 37–45.

2 Elber, W., "The Significance of Fatigue Crack Closure," *Damage Tolerance in Aircraft Structures*, ASTM STP 486, 1971, pp. 230–242.

3 Newman, J. C., Jr., "A Finite-Element Analysis of Fatigue Crack Closure," *Mechanics of Crack Growth*, ASTM STP 590, 1976, pp. 281–301.

4 Ohji, K., Ogura, K., and Ohkubo, Y., "Cyclic Analysis of a Propagating Crack and Its Correlation With Fatigue Crack Growth," *Engineering Fracture Mechanics*, Vol. 7, 1975, pp. 457–464.

5 Ogura, K., and Ohji, K., "FEM Analysis of Crack Closure and Delay Effect in Fatigue Crack Growth Under Variable Amplitude Loading," *Engineering Fracture Mechanics*, Vol. 9, 1977, pp. 471–480.

6 Hanel, J. J., "Rissfortschreitung in ein- und mehrstufig schwingbelasteten Scheiben mit besonderer Berucksichtigung des partiellen Ris-Schliessens," Heft 27, Veroffentlichungen des Instituts fur Statik und Stahlbau der Technischen Hochschule Darmstadt, 1975.

7 Dill, H. D., and Satt, C. R., "Spectrum Crack Growth Prediction Method Based on Crack Surface Displacement and Contact Analysis," MCAIR 75-007, McDonnell Aircraft Company, 1975.

8 Dill, H. D., and Satt, C. R., "Analysis of Crack Growth Following Compressive High Loads Based on Crack Surface Displacements and Contact Analysis," MCAIR 76-006, McDonnell Aircraft Company, 1976.

9 Paris, P. C., and Hermann, L., "Measurements and Analytical Models for Crack Closure in Fatigue," paper presented at 14th International Congress on Theoretical and Applied Mechanics, Delft, 1976.

10 Rice, J. R., "Mechanics of Crack-Tip Deformation and Extension by Fatigue," *Fatigue Crack Propagation*, ASTM STP 415, 1967, p. 247.
11 Rice, J. R., "Mathematical Analysis in the Mechanics of Fracture," Chapter 3 in *Fracture*, Vol. II, ed., Liebowitz, H., Academic Press, 1968.
12 McEvily, A. J., *The Microstructure and Design of Alloys*, The Metals Society, London, 1974, p. 204.